Depolarization after resonance energy transfer (DARET): A sensitive fluorescence-based assay for botulinum neurotoxin protease activity

Marcella A. Gilmore [a], Dudley Williams [a], Yumiko Okawa [a], Bret Holguin [a], Nicholas G. James [b], Justin A. Ross [b], K. Roger Aoki [a], David M. Jameson [b], Lance E. Steward [a,*]

[a] Neurotoxin Research Program, Department of Biological Sciences, Allergan, Irvine, CA 92612, USA
[b] Department of Cell and Molecular Biology, John A. Burns School of Medicine, University of Hawaii, Honolulu, HI 96813, USA

ARTICLE INFO

ABSTRACT

The DARET (depolarization after resonance energy transfer) assay is a coupled Förster resonance energy transfer (FRET)–fluorescence polarization assay for botulinum neurotoxin type A or E (BoNT/A or BoNT/E) proteolytic activity that relies on a fully recombinant substrate. The substrate consists of blue fluorescent protein (BFP) and green fluorescent protein (GFP) flanking SNAP-25 (synaptosome-associated protein of 25 kDa) residues 134–206. In this assay, the substrate is excited with polarized light at 387 nm, which primarily excites the BFP, whereas emission from the GFP is monitored at 509 nm. Energy transfer from the BFP to the GFP in the intact substrate results in a substantial depolarization of the GFP emission. The energy transfer is eliminated when the fluorescent domains separate on cleavage by the endopeptidase, and emission from the directly excited GFP product fragment is then highly polarized, resulting in an overall increase in polarization. This increase in polarization can be monitored to assay the proteolytic activity of BoNT/A and BoNT/E in real time. It allows determination of the turnover rate of the substrate and the kinetic constants (V_{max} and k_{cat}) based on the concentration of cleaved substrate determined directly from the measurements using the additivity properties of polarization. The assay is amenable to high-throughput applications.

© 2011 Elsevier Inc. All rights reserved.

The catalytic light chain domains of the botulinum neurotoxins (BoNTs)[1] are zinc-dependent metalloproteases that cleave proteins involved in the SNARE (soluble *N*-ethylmaleimide-sensitive fusion attachment protein receptor) complex (for recent reviews, see Refs. [1–6]). BoNT serotypes A and E each cleave a specific peptide bond [7–9] in the SNARE protein SNAP-25 (synaptosome-associated protein of 25 kDa [10]), preventing neurotransmitter release at the neuromuscular junction and leading to paralysis. SNAP-25 is also one of two substrates of BoNT/C1 [11]. Unlike other zinc proteases, the BoNTs require an extended recognition sequence for cleavage as well as more remote exosites for optimal binding and cleavage rates [9,12–19]. We have developed an in vitro assay for quantifying BoNT protease activity that permits inclusion of such an extended substrate sequence. Named the DARET (depolarization after resonance energy transfer) assay, this real-time assay is sensitive, simple to assemble, and amenable to high-throughput applications. What makes the assay unique is the application of resonance energy transfer to alter the polarization of the substrate's fluorescence [20,21]. All of the related assays we are aware of rely either on intensity-based Förster resonance energy transfer (FRET) measurements or on fluorescence polarization (FP) measurements, whereas the DARET assay relies on a combination of the two phenomena. Although the principles underlying both FP and FRET are well understood, this appears to be the first instance in which the two have been combined to create a new type of assay. The details of the photophysics underlying the DARET assay are delineated in an accompanying article [22].

FRET involves the nonradiative transfer of energy from a donor to an acceptor molecule following excitation of the donor molecule by incident radiation [20,21,23,24]. The acceptor molecule is raised to an excited state by the energy transfer and then fluoresces at a longer wavelength, returning to its ground state. The efficiency with which this transfer takes place is strongly dependent on several factors, including the spatial separation and relative orientation of the fluorophores and their spectral overlap. Changes in
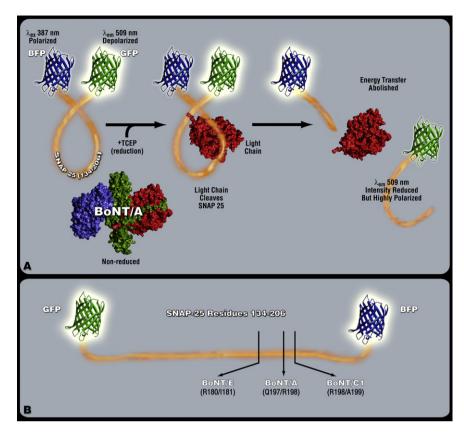
* Corresponding author.
   E-mail address: steward_lance@allergan.com (L.E. Steward).
[1] *Abbreviations used:* BoNT, botulinum neurotoxin; SNARE, soluble *N*-ethylmaleimide-sensitive fusion attachment protein receptor; SNAP-25, synaptosome-associated protein of 25 kDa; DARET, depolarization after resonance energy transfer; FRET, Förster resonance energy transfer; FP, fluorescence polarization; GFP, green fluorescent protein; BFP, blue fluorescent protein; GS25B, GFP–SNAP25(134–206)–BFP; UV–Vis, ultraviolet–visible; MS, mass spectrometry; LC, liquid chromatography; UPLC, ultra-performance liquid chromatography; FA, formic acid; MeCN, acetonitrile; rLC/A, recombinant type A light chain; TCEP, tris(2-carboxyethyl)phosphine; PMT, photomultiplier tube.

Fig.1. (A) DARET assay scheme. The BFP domain of the DARET assay substrate is excited with polarized light at 387 nm. In the intact substrate, the BFP and GFP domains are in close proximity and the GFP is excited by resonance energy transfer from the BFP. The orientation of the GFP relative to the BFP is such that the light emitted by the GFP (509 nm) following the energy transfer is depolarized (black circles in Fig. 2). The energy transfer is abolished after the SNAP-25 segment is cleaved by BoNT endopeptidase and the two fluorescent domains move apart. However, a small amount of direct excitation of the GFP still occurs (at 387 nm), and in this case the emitted light is highly polarized. As more of the substrate molecules are cleaved during the course of an assay, the polarization of the emitted light increases (see Fig. 2). (B) DARET substrate GFP–SNAP25–BFP. The DARET substrate (represented here with the N terminal to the left) is a fully recombinant fusion protein that contains cleavage sites for BoNT/A, BoNT/C1, and BoNT/E; type C1 also cleaves the SNARE protein syntaxin as its primary target.

any or all of these properties result in a change in the measured FRET efficiency. Because the transfer is highly distance dependent, changes in the fluorescence of the donor and acceptor molecules are used in FRET assays to detect changes in their proximity, often brought about by, for example, enzymatic activity. Similarly, changes in these properties can alter the FP. FP is a technique that involves the detection of changes in the polarization of emitted light that can arise from differences in the effective molar volume of reactants and products. Changes in the orientation of a fluorescent molecule (or, more properly, of its dipole moment) between the time it is excited by polarized light and the time it emits light in returning to its ground state lead to depolarization of the emitted light. An increase in the motion of the molecule leads to greater depolarization, whereas a decrease leaves the emitted light more highly polarized. In a standard FP assay, a single small fluorescent molecule becomes attached to or detached from a partner of much greater size, and the polarization of the emitted light increases or decreases correspondingly (see Ref. [25] for a recent review of FP and FP-based assays).

As stated above, the DARET assay combines aspects of both FRET and FP (Fig. 1A). It relies on a recombinant substrate consisting of SNAP-25 residues 134–206 flanked by a green fluorescent protein (GFP) at the N terminus and a blue fluorescent protein (BFP) at the C terminus [26–29]. The photophysical characteristics of the DARET substrate, referred to as GS25B (GFP–SNAP25(134–206)–BFP), are described in the accompanying article [22]. Despite the long intervening SNAP-25 segment, the fluorescent protein domains in the intact substrate are in close spacial proximity, allow-

ing efficient resonance energy transfer. The substrate can, therefore, be used in a standard FRET assay with BFP as the donor and GFP as the acceptor fluorophore. Similar substrates have been reported for FRET assays of BoNT activity both in vitro and in situ [30]. We have not applied the substrate in an FP assay because the change in polarization on proteolysis by BoNT does not provide the dynamic range required for our research [22]. However, with this substrate, we can take advantage of the energy transfer between donor and acceptor that also leads to depolarization of the light emitted by the acceptor molecule. In the DARET assay, the BFP domain of the substrate is excited with polarized light at 387 nm, and the polarization of the light subsequently emitted by the GFP domain at 509 nm is measured. In the intact substrate, the emitted light has a very low (near zero) polarization value. On cleavage by BoNT, the energy transfer is abolished, yet there remains some direct excitation of the GFP product fragment, and the emission from this directly excited GFP is highly polarized. In assay reactions where essentially all of the substrate is cleaved, the change in polarization is approximately 335 mP units.

Materials and methods

Materials

Native BoNT/A dichain was purchased from Metabiologics. Plasmids pQBI T7–BFP and pQBI T7–GFP were purchased from QBiogene. UNO Q6 columns were obtained from Bio-Rad. Bacterial

lysis reagents and metal affinity chromatography resins were purchased from Promega and EMD Chemicals. Tween 20 containing butylhydroxytoluene (BHT) as an antioxidant was purchased from Sigma–Aldrich. All other chemicals were molecular biology grade or the highest purity available.

Substrate coding plasmid

Plasmid pQBI GPF–SNAP25–BFP encodes SNAP-25 residues 134–206, with short linkers at each end, flanked by the GFP and BFP domains. A polyhistidine tag is encoded following the BFP region. The coding DNA and amino acid sequences are included in the supplementary material. The pQBI T7–GFP vector was first modified to include the SNAP-25 segment and a C-terminal polyhistidine tag. The BFP coding region (minus the initiator methionine) was then amplified from the pQBI T7–BFP plasmid and subcloned into the vector between the SNAP-25 segment and the polyhistidine tag.

Protein expression

Freezer stocks of Escherichia coli BL21(DE3) cells containing the pQBI GFP–SNAP25–BFP plasmid were used to inoculate 1-ml starter cultures in PA 0.5G (100 µg/ml ampicillin) medium [31]. The starter cultures were incubated overnight with shaking at 37 °C. These cultures were in turn used at 1000× dilution to inoculate larger expression cultures in prewarmed ZYP-5052 (100 µg/ml ampicillin) autoinduction medium [31]. The ZYP-5052 cultures were grown at 37 °C and 250 rpm for 4 h following inoculation, at which time the temperature was reduced and the cultures were incubated for 18–19 h at 18 °C and 250 rpm. The protein must be expressed below 30 °C for the fluorophores to form properly [32]. Cells from expression cultures were collected by centrifugation (15 min, 6000 RCF, 4 °C) and stored at −80 °C.

Protein purification

All steps were undertaken at 4 °C or on ice except for the cell lysis. Cell paste from a 500-ml expression culture was defrosted on ice and resuspended in 30 ml of room temperature 2× lysis buffer (2× FastBreak cell lysis reagent containing 50 U/ml Benzonase nuclease, 2 kU/ml rLysozme, and 2× Protease Inhibitor Cocktail III). After the cells were resuspended, the final volume was brought to 60 ml with distilled water (dH$_2$O) and the solution was incubated for 30 min at room temperature with gentle rocking. The lysate solution was then clarified by centrifugation for 15 min at 27,000 RCF and 4 °C.

The clarified lysate was applied to a 25-ml metal affinity resin column (either Co^{2+} or Ni^{2+}) at a flow rate of approximately 0.75–1.0 ml/min. The column was washed with 6 column volumes of wash buffer (25 mM Hepes [pH 7.5], 500 mM NaCl, and 10 mM imidazole), and the protein was eluted with 2 column volumes of elution buffer (25 mM Hepes [pH 7.5], 500 mM NaCl, and 500 mM imidazole). The green elution fractions were combined and then concentrated and exchanged into anion exchange buffer A (25 mM Tris–HCl, pH 7.4) in centrifugal concentrators.

An additional anion exchange purification step was accomplished on a UNO Q6 column (Bio-Rad) with buffers that were prechilled and kept on ice throughout the chromatographic procedure. Two chromatographic runs were required; in each, one half of the concentrated sample was applied to the column at a flow rate of 2 ml/min in anion exchange buffer A (50 mM Tris–HCl, pH 7.4). Bound proteins were eluted at a flow rate of 5 ml/min by NaCl gradient in anion exchange buffer B (50 mM Tris–HCl [pH 7.4] and 1 M NaCl) as follows: 7% buffer B for 30 min, 7–15% buffer B over 100 ml, and 100% buffer B for 12 ml at 5 ml/min. Elution of material from

the column was detected by a Bio-Rad QuadTec UV–Vis (ultraviolet–visible) detector at 280 nm, with target protein eluting during the gradient in a broad peak centered at an apparent concentration of 100 mM NaCl. Fractions containing the target protein were combined and then concentrated in Amicon Ultra centrifugal filter devices (50,000 MWCO [molecular weight cutoff], Millipore) and desalted using the same Amicon Ultra centrifugal filter devices or by fast protein liquid chromatography (FPLC) (Bio-Rad Biologic DuoLogic QuadTec UV–Vis detector) with a HiPrep 26/10 size exclusion column (Pharmacia) and an isocratic mobile phase of chilled desalting buffer (25 mM Hepes, pH 7.2, 4 °C) at a flow rate of 10 ml/min.

Liquid chromatography–mass spectrometry analysis

The instrument employed for mass spectrometry (MS) analysis was a Waters–Micromass qTOF (quadrupole time-of-flight) Premier instrument. Proteins were separated prior to MS analysis using a Waters Acquity UPLC (ultra-performance liquid chromatography) system. The separations were performed on a Waters C4 300-Å BEH column operating at 55 °C with a 20-min linear gradient from 0.1% aqueous formic acid (FA) to 0.1% FA in acetonitrile (MeCN). In all cases, the samples were injected at approximately 1–10 pmol of protein on the column without any prior cleanup processes.

General procedure for DARET assays

Native BoNT/A or recombinant type A light chain (rLC/A) was diluted to twice the desired reaction concentration range with 2× reaction buffer (100 mM Hepes [pH 7.2], 0.2% [v/v] Tween 20, and 4 mM tris(2-carboxyethyl)phosphine [TCEP], with or without 20 µM ZnCl$_2$). The diluted samples were added in 20-µl aliquots to wells in a 96-well HE microplate (Molecular Devices), and these reactions were run in triplicate. Each sample was preincubated in 2× reaction buffer at 37 °C for 20–30 min. Prior to initiation of the reactions, the GS25B substrate was diluted with sterile doubly distilled water (ddH$_2$O) to 1.3 µM and warmed to 37 °C. Reactions were initiated by the addition of 20 µl substrate to each well containing endopeptidase. The final concentration of substrate was 0.65 µM unless otherwise indicated. The reaction plates were incubated at 37 °C in a SpectraMax M5 spectrophotometer (Molecular Devices). The polarization of the samples was measured beginning at 5 min following initiation of the reactions and then at 5-min intervals throughout the reaction period (λ_{ex} = 387 nm, λ_{em} = 509 nm, 495-nm cutoff filter, photomultiplier tube [PMT] at 575 V, 11 reads/well). To excite below 400 nm on this spectrophotometer, the program controls must be overridden because the transmission of the polarizing filter decreases sharply at shorter wavelengths. As discussed in the accompanying article [22], if a general-purpose spectrofluorimeter is being used (as opposed to a microplate reader that does not always have the same flexibility) to maximize the change in FP on proteolysis, as well as sensitivity due to light absorption, the substrate should be excited near 375 nm and emission greater than 510 nm should be collected.

Enzyme kinetics of rLC/A and 150-kDa native BoNT/A with the GS25B substrate

Kinetic parameters were determined using a series of concentrations of GS25B (0.15, 0.3, 0.6, 0.8, 1, 1.5, 2.5, 5, and 10 µM for rLC/A; 0.15, 0.3, 0.6, 0.8, 1, 1.5, and 3.5 µM for 150-kDa native BoNT/A) titrated with either rLC/A (5 nM) or reduced BoNT/A (1 nM) at 37 °C. The polarization measurements were conducted on an ISS PC1 spectrofluorimeter exciting at 375 nm and collecting emission at wavelengths greater than 525 nm through a 537-nm

longpass filter (Corning, product no. 3484). The concentration of cleaved substrate was calculated using the additivity of polarization, incorporating the correction for the change of intensity on proteolysis [33]:

$$\left(\frac{1}{P_{obs}} - \frac{1}{3}\right)^{-1} = \sum f_i \left(\frac{1}{P_i} - \frac{1}{3}\right)^{-1}, \tag{1}$$

where P_{obs} is the observed polarization and f_i and P_i are the fractional intensity of the emission and polarization of the ith component, respectively. The emission detected is proportional to the concentration of the ith species via the relation $f_i = F_i C_i / I$, where F_i is fluorescence intensity per unit concentration C_i and the total fluorescence intensity $I = \sum F_i C_i$. The values of F_i for the intact and cleaved substrate are determined from the total fluorescence intensity ($I_{parallel} + 2I_{perpendicular}$) prior to the addition of the protease and on 100% proteolysis of the substrate, respectively. To calculate the fraction of cleaved substrate, one must take into account the change in intensity on proteolysis (i.e., the cleaved substrate is approximately one-fifth as bright as the intact substrate). The fraction cleaved (f_c), in terms of the polarization of the intact (P_{int}), cleaved (P_c) and observed (P_{obs}) and the enhancement (g) of the intensity on cleavage ($g = F_{cleaved}/F_{intact}$), is given by Eq. (2) [25]:

$$f_c = \frac{(P_{int} - P_{obs})(3 - P_c)}{g(P_{obs})(3 - P_{int}) + (P_{int} - P_{obs})(3 - P_c)}. \tag{2}$$

The initial linear change in fraction cleaved (10–25%) was fit to obtain rate constants at each substrate concentration. Multiplication of these rate constants with the initial ($t = 0$ s) substrate concentration converts the units of these rates to concentration of product formation over time ($\mu M\ s^{-1}$). K_M and k_{cat} were determined from simple Michaelis–Menten kinetics using custom scripts written in MATLAB.

Results and discussion

Substrates for assays of BoNT/A and BoNT/E proteolytic activity require an extended recognition sequence to achieve the best binding characteristics. Short peptides, although easy to produce synthetically, have poor K_M values [12,14,16–19]. SNAP-25, the natural target of these BoNTs, contains 206 amino acids [10]. Selection of the 73 C-terminal residues (134–206) for inclusion in the DARET substrate (GS25B) (Fig. 1B) was made based on the biochemical information available at the time regarding BoNT/A substrate requirements as well as SNAP-25 structural characteristics. This fragment includes a SNARE recognition motif [15] and is within the region that forms the C-terminal α-helix of SNAP-25 in the SNARE complex [34]. The BoNT/A, BoNT/C1, and BoNT/E cleavage sites within the SNAP-25 sequence are Gln197/Arg198 for type A [8,9,35], Arg198/Ala199 for type C1 [11,18], and Arg180/Ile181 for type E [7].

Although the GS25B substrate can be employed in a FRET intensity ratio assay (similar to Dong et al. [30]), there are advantages to combining resonance energy transfer with FP. By relying on energy transfer to depolarize the emissions in an intact substrate, the relative size and lifetime of the acceptor fluorophore, or of the molecule to which it is attached, becomes less important. In addition, measuring the fluorescence only from the acceptor molecule reduces the background noise when working in complex biological matrices that autofluoresce. Molecules excited at the donor fluorophore's excitation wavelength are unlikely to fluoresce at the emission maximum of the acceptor fluorophore. These unique features of the DARET assay have allowed us to exploit a fully recombinant substrate in which the change in effective molar volume on proteolysis is not great enough to be generally useful in a standard FP assay. Furthermore, we are able to measure BoNT proteolytic activ-

Table 1
MS analysis of GS25B.

Identity	Expected mass (Da)	Observed mass (Da)	Δ Mass[a] (Da)
Intact GS25B	63,824	63,823	1
N-terminal LC/A cleavage fragment	34,884	34,884	0
C-terminal LC/A cleavage fragment	28,958	28,958	0

[a] Following protein expression, the GFP and BFP domains become chemically modified and photochemically active in a maturation process. The expected mass was calculated based on the photochemically mature protein.

ity in crude cell lysates with low levels of background interference. Although the DARET assay substrate was designed for cell-free work, a DARET-type assay could be applied in cells. If autofluorescence is a problem, a red-shifted pair of fluorescent proteins should reduce such interference. Another option is to employ a homo-FRET pair, an alternative we are currently testing.

Substrate and enzymatic fragment analysis by LC–MS

The GS25B substrate was analyzed by LC–MS to confirm its identity in terms of its expected mass. In addition, the proteolytic fragments produced on cleavage by rLC/A were analyzed to identify the fragments generated and verify the predicted cleavage site by the fragment masses. The intact GS25B protein provided an observed mass that was within 1 Da of that calculated from its sequence (Table 1), a calculation that includes chemical modifications that are part of the chromophore formation process [27,36,37]. Following proteolysis by rLC/A, formation of two protein fragments was observed along with the disappearance of the starting material. Analysis of the fragments confirmed that the substrate was cleaved at the SNAP-25 Gln197/Arg198 site, with fragment masses identical to those predicted from the sequence (Table 1).

DARET assays of native BoNT/A and analyte screening

BoNTs are approximately 150-kDa proteins composed of three domains: a zinc-dependent metalloprotease at the N terminus followed by translocation and binding domains. Type A is purified from *Clostridia* as a dichain molecule, where the catalytic domain constitutes the 50-kDa light chain endopeptidase and the remainder of the molecule comprises the heavy chain. The chains are linked by a disulfide bond and extensive noncovalent interactions, including a belt region from the heavy chain that wraps around the light chain, occluding the active site [38] as well as other sites important for substrate recognition [13]. The disulfide bond must be reduced so that the belt can move and allow access to the active site before proteolytic activity can be assayed in vitro. To that end, BoNT/A was preincubated in reducing buffer prior to initiation of the DARET assays. The standard assay conditions were selected to allow acquisition of activity data for native BoNT/A over a concentration range from 6 to 800 pM in a 1-h assay. The GS25B substrate was included at a final concentration of 0.65 μM in a total reaction volume of 40 μl and the reactions were incubated at 37 °C, with FP measurements taken at 5-min intervals. Typical progress curves from an assay are shown in Fig. 2. The assay conditions can be modified to suit other research needs, for example, to facilitate overnight incubation of reactions.

Although data are collected over the entire time course of the reactions, the full progress curves for each set of reactions are not typically plotted. Instead, the assay results are graphed for data collected at a set time point for each concentration in the range of
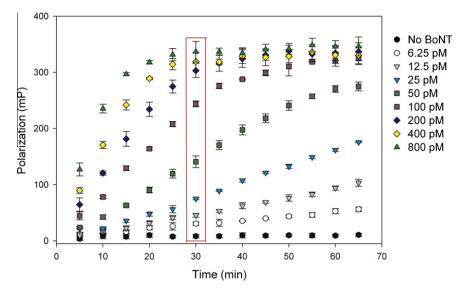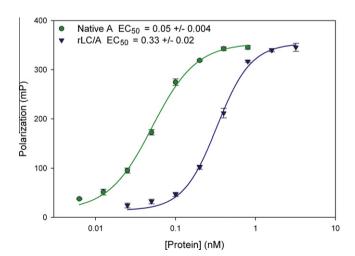
Fig.2. DARET assay progress curves. Typical DARET assay progress curves for the positive control, 150-kDa native BoNT/A, are shown. The full progress curves are not graphed for routine screening assays. Instead, data from the 30-min time points (red box) are graphed for analysis (see Fig. 3). mP, Millipolarization units.

endopeptidase concentrations assayed, allowing calculation of EC_{50} values for the analytes being tested (Fig. 3). This approach is quick and simple for screening the light chain activity of BoNT/A and BoNT/E and allows the option of analyzing the complete data in greater detail when necessary.

Z'-factor evaluation of the DARET assay yields a Z'-factor [39] of 0.869, which is indicative of a high-quality assay. For this assessment, the positive and negative control data from the assay, in this case the native BoNT/A reactions and the substrate-only reactions to which no endopeptidase was added, were analyzed to ensure that the results were reproducible and that the signal variation was acceptable (see Supplementary material). The positive control value was the polarization measured at the 30-min time point for the reactions containing the highest concentration of native BoNT/

Fig.3. DARET assay of rLC/A. DARET assay of rLC/A over a concentration range of 0.036–4.6 nM relative to native BoNT/A over a concentration range of 0.00625–0.8 nM is shown. These reactions included GS25B substrate at a concentration of 0.5 μM and were incubated at 37 °C for 65 min. The polarization of the samples was measured beginning at 5 min following initiation of the reactions and then at 5-min intervals throughout the reaction period (λ_{ex} = 387 nm, λ_{em} = 509 nm, 495-nm cutoff filter, PMT at 575 V, 11 reads/well). The data from the 30-min time point are graphed. The ratio of the analyte EC_{50} to the native BoNT/A EC_{50} indicates that the catalytic efficiency of the analyte is 6-fold less than that of the native control. mP, Millipolarization units.
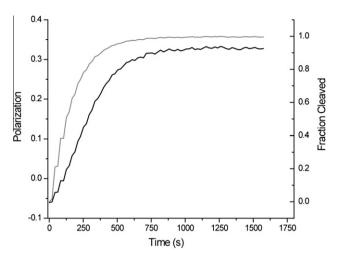
A (800 pM). The negative control value was the polarization measured at the 30-min time point for the substrate-only solutions. An inactive recombinant BoNT/A did not alter the polarization (data not shown), demonstrating that binding did not alter the substrate's fluorescence properties.

Graphing the data collected at a set time point and calculating EC_{50} values for analytes and the native BoNT/A control assayed in each 96-well plate provides a comparative LC/A activity value for each analyte by reporting the ratio of the analyte EC_{50} to the native BoNT/A EC_{50}. The DARET results are graphed with SigmaPlot software, and the curves are fit with a four-parameter logistic equation. The example shown in Fig. 3 is an assay of rLC/A containing N-terminal purification tags [40] that has an EC_{50} of 0.328 nM compared with 0.052 nM for native BoNT/A, yielding an EC_{50} ratio of 6.3. Kinetic analysis of this rLC/A molecule confirmed the 6-fold reduction in catalytic efficiency compared with native BoNT/A (see below).
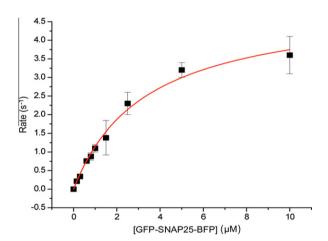
Enzyme kinetics of native BoNT/A and rLC/A

The in vitro assays that have been reported for quantifying BoNT protease activity or screening potential inhibitors of that activity include various immuno-based [41–43], high-performance liquid chromatography (HPLC)/UPLC-based [16,17,44–47], LC–MS-based [48], surface plasmon resonance (SPR)-based [49,50], and capillary electrophoresis-based [51–53] assays, FRET and fluorescence quench relief assays [30,44,54–56], and assays based on fluorescence release from immobilized substrates [57,58]. Lebeda and coworkers [2], in a review of BoNT kinetic studies, noted the large variation in K_M and k_{cat} values reported for BoNT/A and that larger k_{cat}/K_M values were determined from assays where the substrate was full-length SNAP-25 or contained a SNAP-25 fragment at least 61 residues long. The k_{cat}/K_M values determined with a 17-mer fragment of SNAP-25 as the substrate were in the range of 10^2 to 10^3 s^{-1} M^{-1}, whereas the largest ratio in their survey, 3.7×10^6 s^{-1} M^{-1}, was associated with a substrate containing 61 SNAP-25 residues. Poras and coworkers [56] reported that a 48-mer peptide containing norleucines in place of methionines yielded a k_{cat}/K_M value of 8.85×10^6 s^{-1} M^{-1}. Kinetic assays with the DARET substrate agree with these findings.

The fraction of the GS25B substrate cleaved, and therefore the kinetic parameters K_M and k_{cat}, can be determined by monitoring

Fig.4. Kinetic trace of proteolysis of 300 nM GFP–SNAP25–BFP by 5 nM rLC/A at 37 °C followed by polarization (black). The fraction cleaved is also shown (gray).

Fig.5. Kinetics of GFP–SNAP25–BFP cleavage by rLC/A. The concentration-dependent initial rates versus substrate (S) concentration are fit to a hyperbola, $k_{cat}[S]/(K_m + [S])$, to determine the steady-state kinetic constants k_{cat} and K_M.

the FP change during assays of BoNT proteolytic activity (as described in Materials and Methods). Fig. 4 shows a typical progress curve for the cleavage of GS25B with rLC/A and the fraction of the substrate cleaved using Eq. (2), as obtained on a standard steady-state fluorimeter. On this instrument, the values of F_{intact} and $F_{cleaved}$ were 1,230,000 and 281,000 counts/s/μM, respectively, and the polarizations of the intact and cleaved substrate were −0.043 and 0.335, respectively. The kinetic parameters determined from Michaelis–Menten analysis of the kinetic plots (Fig. 5) for rLC/A and 150-kDa native BoNT/A are presented in Table 2. The basis of the difference in catalytic efficiency between the two molecules is explained by these parameters. With an identical proteolytic mechanism for both molecules, the turnover rates (k_{cat}) were pre-

Table 2
Kinetic constants of rLC/A and 150-kDa native BoNT/A.

Protein	K_M (μM)	k_{cat} (s^{-1})	k_{cat}/K_M (μM^{-1} s^{-1})
rLC/A	3.4 ± 0.3	5.0 ± 0.4	1.4 ± 0.1
150-kDa BoNT/A	0.51 ± 0.07	4.5 ± 0.2	8.8 ± 0.2

Note: All data were recorded at 37 °C. Values presented are means ± standard deviations ($n \geqslant 2$).

dicted to be nearly equal, a prediction that our results validate. However, there is a 6-fold higher catalytic efficiency for the native BoNT/A compared with the recombinant light chain as a result of a tighter association, K_M (Table 2). The additional protein sequence included at the N terminus of the rLC/A molecule is probably responsible for its reduced substrate affinity given that the N terminus is near the extended substrate binding cleft [13]. LC/A activity appears to be sensitive to the exact sequence of the light chain, as demonstrated by other assays [40].

Conclusion

In this article, we have described a fluorescence-based assay for the protease activity of BoNT/A or BoNT/E. This assay, termed DARET, uses a substrate containing SNAP-25 residues 134–206 linked to BFP and GFP. The assay takes advantage of the fact that FRET between the donor (BFP) and acceptor (GFP) moieties results in significant depolarization of the emission, which is subsequently abolished after cleavage of the substrate separates the donor and acceptor. The assay is versatile, allowing high-throughput screening with rapid data acquisition and analysis as well as characterization such as determination of Michaelis–Menten parameters (i.e., K_m and V_{max}) for BoNT/A and BoNT/E.

The application of resonance energy transfer to alter the polarization of emitted light provides several advantages, including a reduction in background interference in DARET measurements compared with intensity-based FRET assays. This background reduction occurs because the endogenous fluorophores in more complex biological mixtures, such as *E. coli* lysates, do not have Stokes shifts as large as the difference between the excitation and emission wavelengths of the DARET assay. This fact allows direct testing for BoNT light chain activity in crude cell lysates. Other advantages include the absolute nature of the measurement, which does not rely on the particular instrument platform used, and the ability to calculate the fraction of substrate cleaved directly from the FP measurements, which simplifies kinetic analyses and would allow application of DARET as an absolute assay. In contrast, intensity-based FRET assays will produce different intensity ratios depending on the precise instrumentation employed and generally require a standard curve as a reference to determine the extent of proteolysis. The DARET assay can be applied to other proteases by altering the amino acid sequence separating the two fluorophores to include the substrate sequence for the desired protease.

Appendix A. Supplementary data

Supplementary data associated with this article can be found, in the online version, at doi:10.1016/j.ab.2011.01.043.

References

[1] T. Binz, S. Sikorra, S. Mahrhold, Clostridial neurotoxins: mechanism of SNARE cleavage and outlook on potential substrate specificity reengineering, Toxins 2 (2010) 665–682.
[2] F.J. Lebeda, R.Z. Cer, U. Mudunuri, R. Stephens, B.R. Singh, M. Adler, The zinc-dependent protease activity of the botulinum neurotoxins, Toxins 2 (2010) 978–997.
[3] M. Montal, Botulinum neurotoxin: a marvel of protein design, Annu. Rev. Biochem. 79 (2010) 591–617.
[4] M.R. Popoff, P. Bouvet, Clostridial toxins, Future Microbiol. 4 (2009) 1021–1064.

[5] B. Poulain, M.R. Popoff, J. Molgo, How do the botulinum neurotoxins block neurotransmitter release: from botulism to the molecular mechanism of action, Botulinum J. 1 (2008) 14–87.

[6] O. Rossetto, L. Morbiato, P. Caccin, M. Rigoni, L. Carli, M. Paoli, M. Cintra-Francischelli, C. Montecucco, Tetanus, botulinum, and snake presynaptic neurotoxins, Rendiconti Lincei 19 (2008) 173–188.

[7] T. Binz, J. Blasi, S. Yamasaki, A. Baumeister, E. Link, T.C. Sudhof, R. Jahn, H. Niemann, Proteolysis of SNAP-25 by types E and A botulinal neurotoxins, J. Biol. Chem. 269 (1994) 1617–1620.

[8] J. Blasi, E.R. Chapman, E. Link, T. Binz, S. Yamasaki, P. De Camilli, T.C. Sudhof, H. Niemann, R. Jahn, Botulinum neurotoxin A selectively cleaves the synaptic protein SNAP-25, Nature 365 (1993) 160–163.

[9] G. Schiavo, O. Rossetto, S. Catsicas, P. Polverino de Laureto, B.R. DasGupta, F. Benfenati, C. Montecucco, Identification of the nerve terminal targets of botulinum neurotoxin serotypes A, D, and E, J. Biol. Chem. 268 (1993) 23784–23787.

[10] G.A. Oyler, G.A. Higgins, R.A. Hart, E. Battenberg, M. Billingsley, F.E. Bloom, M.C. Wilson, The identification of a novel synaptosomal-associated protein, SNAP-25, differentially expressed by neuronal subpopulations, J. Cell Biol. 109 (1989) 3039–3052.

[11] P. Foran, G.W. Lawrence, C.C. Shone, K.A. Foster, J.O. Dolly, Botulinum neurotoxin C1 cleaves both syntaxin and SNAP-25 in intact and permeabilized chromaffin cells: correlation with its blockade of catecholamine release, Biochemistry 35 (1996) 2630–2636.

[12] S.A. Ahmed, M.A. Olson, M.L. Ludivico, J. Gilsdorf, L.A. Smith, Identification of residues surrounding the active site of type A botulinum neurotoxin important for substrate recognition and catalytic activity, Protein J. 27 (2008) 151–162.

[13] M.A. Breidenbach, A.T. Brunger, Substrate recognition strategy for botulinum neurotoxin serotype A, Nature 432 (2004) 925–929.

[14] S. Chen, J.T. Barbieri, Unique substrate recognition by botulinum neurotoxins serotypes A and E, J. Biol. Chem. 281 (2006) 10906–10911.

[15] O. Rossetto, G. Schiavo, C. Montecucco, B. Poulan, L. Lozzi, C.C. Shone, SNARE motif and neurotoxins, Nature 372 (1994) 415–416.

[16] J.J. Schmidt, K.A. Bostian, Proteolysis of synthetic peptides by type A botulinum neurotoxin, J. Protein Chem. 14 (1995) 703–708.

[17] J.J. Schmidt, K.A. Bostian, Endoproteinase activity of type A botulinum neurotoxin: substrate requirements and activation by serum albumin, J. Protein Chem. 16 (1997) 19–26.

[18] V.V. Vaidyanathan, K. Yoshino, M. Jahnz, C. Dorries, S. Bade, S. Nauenburg, H. Niemann, T. Binz, Proteolysis of SNAP-25 isoforms by botulinum neurotoxin types A, C, and E: domains and amino acid residues controlling the formation of enzyme–substrate complexes and cleavage, J. Neurochem. 72 (1999) 327–337.

[19] P. Washbourne, R. Pellizzari, G. Baldini, M.C. Wilson, C. Montecucco, Botulinum neurotoxin types A and E require the SNARE motif in SNAP-25 for proteolysis, FEBS Lett. 418 (1997) 1–5.

[20] E. Gaviola, P. Pringsheim, Über den Einfluss der Konzentration auf die Polarisation der Fluoreszenz von Farbstofflösungen, Z. Physik. 24 (1924) 24–36.

[21] G. Weber, Fluorescence-polarization spectrum and electronic-energy transfer in tyrosine, tryptophan, and related compounds, Biochem. J. 75 (1960) 335–345.

[22] J.A. Ross, M.A. Gilmore, D. Williams, K.R. Aoki, L.E. Steward, D.M. Jameson, Characterization of Förster resonance energy transfer in a botulinum neurotoxin assay, Anal. Biochem. (2011).

[23] J.F. Eccleston, J.P. Hutchinson, D.M. Jameson, Fluorescence-based assays, Prog. Med. Chem. 43 (2005) 19–48.

[24] B. Valeur, Molecular Fluorescence: Principles and Applications, Wiley–VCH, Weinheim, Germany, 2006.

[25] D.M. Jameson, J.A. Ross, Fluorescence polarization/anisotropy in clinical diagnostics and imaging, Chem. Rev. 110 (2010) 2685–2708.

[26] A.B. Cubitt, R. Heim, S.R. Adams, A.E. Boyd, L.A. Gross, R.Y. Tsien, Understanding, improving, and using green fluorescent proteins, Trends Biol. Sci. 20 (1995) 448–455.

[27] R. Heim, D.C. Prasher, R.Y. Tsien, Wavelength mutations and posttranslational autoxidation of green fluorescent protein, Proc. Natl. Acad. Sci. USA 91 (1994) 12501–12504.

[28] D.C. Prasher, V.K. Eckenrode, W.W. Ward, F.G. Prendergast, M.J. Cormier, Primary structure of the Aequorea victoria green fluorescent protein, Gene 111 (1992) 229–233.

[29] O. Shimomura, F.H. Johnson, Y. Saiga, Extraction, purification, and properties of aequorin, a bioluminescent protein from the luminous hydromedusan, Aequorea, J. Cell. Comp. Physiol. 59 (1962) 223–239.

[30] M. Dong, W.H. Tepp, E.A. Johnson, E.R. Chapman, Using fluorescent sensors to detect botulinum neurotoxin activity in vitro and in living cells, Proc. Natl. Acad. Sci. USA 101 (2004) 14701–14706.

[31] F.W. Studier, Protein production by auto-induction in high density shaking cultures, Protein Expr. Purif. 41 (2005) 207–234.

[32] M. Zimmer, Green fluorescent protein (GFP): applications, structure, and related photophysical behavior, Chem. Rev. 102 (2002) 759–781.

[33] G. Weber, Polarization of the fluorescence of macromolecules: I. Theory and experimental method, Biochem. J. 51 (1952) 145–155.

[34] R.B. Sutton, D. Fasshauer, R. Jahn, A.T. Brunger, Crystal structure of a SNARE complex involved in synaptic exocytosis at 2.4 Å resolution, Nature 395 (1998) 347–353.

[35] G. Schiavo, C.C. Shone, O. Rossetto, F.C. Alexander, C. Montecucco, Botulinum neurotoxin serotype F is a zinc endopeptidase specific for VAMP/synaptobrevin, J. Biol. Chem. 268 (1993) 11516–11519.

[36] R.M. Wachter, Chromogenic cross-link formation in green fluorescent protein, Acc. Chem. Res. 40 (2007) 120–127.

[37] L. Zhang, H.N. Patel, J.W. Lappe, R.M. Wachter, Reaction progress of chromophore biogenesis in green fluorescent protein, J. Am. Chem. Soc. 128 (2006) 4766–4772.

[38] D.B. Lacy, W. Tepp, A.C. Cohen, B.R. DasGupta, R.C. Stevens, Crystal structure of botulinum neurotoxin type A and implications for toxicity, Nat. Struct. Biol. 5 (1998) 898–902.

[39] J.H. Zhang, T.D. Chung, K.R. Oldenburg, A simple statistical parameter for use in evaluation and validation of high throughput screening assays, J. Biomol. Screen. 4 (1999) 67–73.

[40] E. Fernandez-Salas, L.E. Steward, H. Ho, P.E. Garay, S.W. Sun, M.A. Gilmore, J.V. Ordas, J. Wang, J. Francis, K.R. Aoki, Plasma membrane localization signals in the light chain of botulinum neurotoxin, Proc. Natl. Acad. Sci. USA 101 (2004) 3208–3213.

[41] T.A. Ekong, I.M. Feavers, D. Sesardic, Recombinant SNAP-25 is an effective substrate for Clostridium botulinum type A toxin endopeptidase activity in vitro, Microbiology 143 (1997) 3337–3347.

[42] B. Hallis, B.A.F. James, C.C. Shone, Development of novel assays for botulinum type A and B neurotoxins based on their endopeptidase activities, J. Clin. Microbiol. 34 (1996) 1934–1938.

[43] R.G.A. Jones, M. Ochiai, Y. Liu, T. Ekong, D. Sesardic, Development of improved SNAP25 endopeptidase immuno-assays for botulinum type A and E toxins, J. Immunol. Methods 329 (2008) 92–101.

[44] C. Anne, F. Cornille, C. Lenoir, B.P. Roques, High-throughput fluorogenic assay for determination of botulinum type B neurotoxin protease activity, Anal. Biochem. 291 (2001) 253–261.

[45] T. Hunt, D. Rupp, G. Shimizu, K. Tam, J. Weidler, J. Xie, Characterization of SNARE cleavage products generated by formulated botulinum neurotoxin type-A drug products, Toxins 2 (2010) 2198–2212.

[46] B. Rowe, J.J. Schmidt, L.A. Smith, S.A. Ahmed, Rapid product analysis and increased sensitivity for quantitative determinations of botulinum neurotoxin proteolytic activity, Anal. Biochem. 396 (2010) 188–193.

[47] N. Shine, L. Eaton, K. Crawford, A continuous fluorimetric assay for high-throughput screening for botulinum toxin type A inhibitors, Naunyn Schmiedebergs Arch. Pharmacol. 365 (2002) R40.

[48] K. Capkova, M.S. Hixon, L.A. McAllister, K.D. Janda, Toward the discovery of potent inhibitors of botulinum neurotoxin A: development of a robust LC–MS based assay operational from low to subnanomolar enzyme concentrations, Chem. Commun. (Camb.) (2008) 3525–3527.

[49] G. Ferracci, R. Miquelis, S. Kozaki, M. Seagar, C. Leveque, Synaptic vesicle chips to assay botulinum neurotoxins, Biochem. J. 391 (2005) 659–666.

[50] S. Marconi, G. Ferracci, M. Berthomieu, S. Kozaki, R. Miquelis, J. Boucraut, M. Seagar, C. Leveque, A protein chip membrane-capture assay for botulinum neurotoxin activity, Toxicol. Appl. Pharmacol. 233 (2008) 439–446.

[51] M. Adler, H.F. Shafer, H.A. Manley, B.E. Hackley Jr., J.D. Nicholson, J.E. Keller, M.C. Goodnough, A capillary electrophoresis technique for evaluating botulinum neurotoxin B light chain activity, J. Protein Chem. 22 (2003) 441–448.

[52] T.D. Laing, A.J. Marenco, D.M. Moore, G.J. Moore, D.C. Mah, W.E. Lee, Capillary electrophoresis laser-induced fluorescence for screening combinatorial peptide libraries in assays of botulinum neurotoxin A, J. Chromatogr. B 843 (2006) 240–246.

[53] A.L. Purcell, H.M. Hoard-Fruchey, A capillary electrophoresis method to assay catalytic activity of botulinum neurotoxin serotypes: implications for substrate specificity, Anal. Biochem. 366 (2007) 207–217.

[54] E.A. Perpetuo, L. Juliano, M.A. Juliano, F. Fratelli, S.M. Prado, D.C. Pimenta, I. Lebrun, Enzymatic profiling of tetanus and botulinum neurotoxins based on vesicle-associated membrane protein derived fluorogenic substrates, Protein Pept. Lett. 15 (2008) 1100–1106.

[55] M. Pires-Alves, M. Ho, K.K. Aberle, K.D. Janda, B.A. Wilson, Tandem fluorescent proteins as enhanced FRET-based substrates for botulinum neurotoxin activity, Toxicon 53 (2009) 392–399.

[56] H. Poras, T. Ouimet, S.V. Orng, M.C. Fournie-Zaluski, M.R. Popoff, B.P. Roques, Detection and quantification of botulinum neurotoxin type A by a novel rapid in vitro fluorimetric assay, Appl. Environ. Microbiol. 75 (2009) 4382–4390.

[57] H.B. Hines, A.D. Kim, R.G. Stafford, S.S. Badie, E.E. Brueggeman, D.J. Newman, J.J. Schmidt, Use of a recombinant fluorescent substrate with cleavage sites for all botulinum neurotoxins in high-throughput screening of natural product extracts for inhibitors of serotypes A, B, and E, Appl. Environ. Microbiol. 74 (2008) 653–659.

[58] J.J. Schmidt, R.G. Stafford, C.B. Millard, High-throughput assays for botulinum neurotoxin proteolytic activity: serotypes A, B, D, and F, Anal. Biochem. 296 (2001) 130–137.